Farraday Johnson earned her B.S. in Biomedical Engineering with a minor in Chemistry from the University of Memphis in the Fall of 2024, where she was an Emerging Leader Scholar and Urban STEM Scholar. She began research as a Helen Hardin Honors College Summer Fellow, studying dual drug delivery, and later participated in the UTHSC and UPenn STAR research programs, focusing on Alzheimer's Disease and Related Dementias. As an undergraduate, she conducted ultrasound research in Dr. Carl Herickhoff's lab, presenting at the International Symposium for Ultrasonic Imaging and Tissue Characterization and earning 1st place at the University of Memphis's Student Research Forum. Now a Clinical Research Coordinator at the University of Pennsylvania, Farraday aspires to become a neurologist and is passionate about advancing Alzheimer's disease research.

Carl Herickhoff was born in Mankato, MN, in 1982. He earned a B.S. in Electrical Engineering from the University of Notre Dame in 2005, and a Ph.D. in Biomedical Engineering from Duke University in 2011. His professional career in ultrasound devices and systems research has included time at GE Global Research Center, Philips, Healthcare, Duke University, and Stanford University, before joining the Biomedical Engineering Faculty at the University of Memphis in 2020. Dr. Herickhoff received the NSF CAREER Award in 2023. His current research interests include transcranial ultrasound blood flow detection, super-resolution functional ultrasound imaging, breast cancer ultrasound screening, and quantitative ultrasound computed tomography techniques.

Farraday Johnson & Carl Herickhoff

Simulation of a 2D Array Transducer Design for Transcranial Doppler Signal Acquisition

Faculty Sponsor

Dr. Carl Herickhoff

Abstract

Timely and accurate diagnosis of strokes is critical for effective treatment to prevent further neuronal cell death and functional impairment. Acquisition of transcranial doppler (TCD) ultrasound signals to detect stroke is challenging due to the need to find an acceptable acoustic window through the skull and intersect the beam with the middle cerebral artery. We investigated the design of a novel 2D array transducer intended to interrogate skull thickness and allow steerability of the ultrasound beam to facilitate TCD signal acquisition. Field II, a MATLAB program that simulates ultrasound transducer fields, was used to model multiple 2D array geometries using triangular transducer elements inscribed within a 2 cm diameter circle. The results obtained suggest that a simplified 2D array transducer could be fabricated to provide TCD users with feedback to aid in optimal signal acquisition.

Introduction

Each year, there are 800,000 strokes in the United States leading to an average of 150,000 deaths, at a cost of $50 billion.[1] A stroke is a disruption of blood flow to the brain, and there are two types of strokes: hemorrhagic and ischemic. Hemorrhagic stroke occurs when there is a leakage of blood to surrounding areas within the brain due to a rupture of a cerebral vessel. Ischemic stroke occurs when there is a blockage of an artery within the brain by a blood clot or vascular plaque. Ischemic strokes account for 87% of strokes, with large-vessel occlusions (LVOs) as the most severe ischemic strokes; LVOs occur in 38% of ischemic stroke cases and account for over 90% of stroke deaths.[1,2]

The accurate identification of stroke type is critical because the treatment for each stroke type would exacerbate the other type. Furthermore, delay in identifying and treating stroke in a timely manner can lead to disability (e.g., physical or cognitive impairment) or death. For instance, ischemic stroke can be treated with tissue plasminogen activator (tPA, a blood thinner), and must be administered within 4.5 hours of onset of the stroke.[3] If a hemorrhagic stroke were to be treated using tPA, bleeding within the surrounding areas of the brain would be exacerbated, possibly leading to further neurologic issues. Currently, stroke type is determined (and LVOs are identified) by computed tomography angiography (CTA).[4]

Transcranial Doppler

Transcranial doppler ultrasonography (TCD) is currently used as an inexpensive way to monitor stroke patients by measuring the blood flow velocity in cerebral arteries.[5] Unlike CTA, TCD does not involve radiopaque contrast dye or ionizing radiation. Current TCD devices consist of a circular single-element transducer that generates a fixed beam, so the user must move the device manually to search for overlap of the beam with a major artery, such as the middle cerebral artery (MCA), to obtain a blood flow signal. To our knowledge, no clinical TCD devices incorporate a non-imaging transducer array. The other challenge for clinical users of this device is locating a sufficient acoustic window—the thinnest region of skull bone that allows optimal ultrasound beam transmission.

Thus, current TCD devices require optimization of four degrees of freedom (translation and rotation about x and y over the temporal region of the head) by trial and error. The goal of this project is to design a simple 2D array to both (1) sample the skull thickness underlying the array area and return a 2D profile to help locate an acoustic window, and (2) elec-

tronically steer the ultrasound receive beam in multiple directions off-axis and return a suggestion of angular tilt to optimize beam-vessel alignment and maximize blood flow signal. This array device would enable unskilled users to quickly and confidently detect the presence or absence of MCA blood flow and rapidly determine when a patient has an LVO stroke.

Methods

6-element array

Unlike current circular single-element or linear-array transducer geometries, a transducer array was fabricated using triangular elements to aid in beam optimization and steering. Utilizing the MATLAB-based Field II ultrasound simulation package, a novel 2D array of triangular elements was designed in **Figure 1**, using six elements inscribed in a 2 cm circle, the approximate diameter of current TCD devices. The sides of the inner triangular elements measured 10 mm each. The kerf, or distance, between each element was 0.04 mm. Beam patterns in the X-Z and Y-Z planes were simulated at focal ranges at 1 cm and 6 cm.

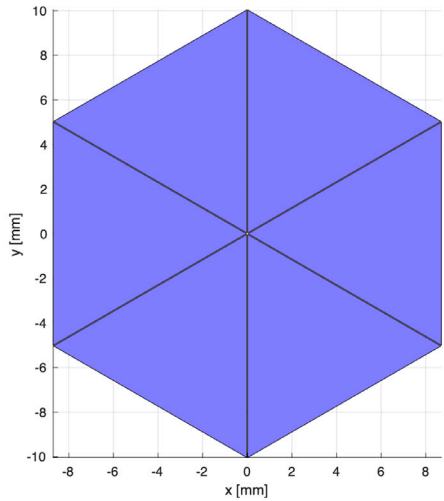

Figure 1.
2D element array consisting of 6 triangular elements

12-element Array

In Figure 2, a 12-element array was similarly configured and inscribed within a 2 cm circle. The sides of each element measured at 5.73 mm. The kerf was set to 0.04 mm. Beam patterns in the X-Z, Y-Z, and X-Y planes were simulated. For the X-Y plane, Z was initially set to 5 mm and then adjusted to the beam maximum. Focal ranges of [1:1:6] cm were simulated. Next, the array apodization (element-by-element weighting) was manipulated so that the response under individual elements was simulated. Apodization was constructed by activating and deactivating select transducer elements to minimize side lobes and modify the beam profile. This addresses the long-term goal of sampling and profiling the skull thickness. Finally, the beam for the whole array was steered off-axis by 10° in the azimuth (X) direction.

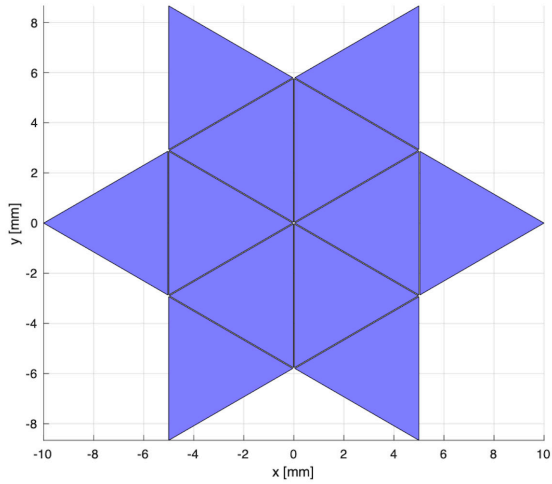

Figure 2.
Novel 2D element array consisting of 12 triangular elements.

Results and Discussion

6-element Array: Focal Range Control for X-Z and Y-Z Planes

In **Figure 3**, the X-Z and Y-Z planes are focused at 1 cm and 6 cm. The 6 cm focal range has a deeper focus; however, as shown in **Figure 3**, there was no observable difference in the beam patterns. This is due to the absence of curvature in the delay profile (only two transducer elements' transmit

timing cannot be phased to generate a concave wavefront converging to a focus). Since only two source points are symmetrically positioned about the origin, the resulting wavefront does not have the curvature necessary for beam focusing. The same occurrence was observed in the orthogonal plane. In summary, a curved delay profile cannot be achieved when an array provides only two elements along a given line through the origin.

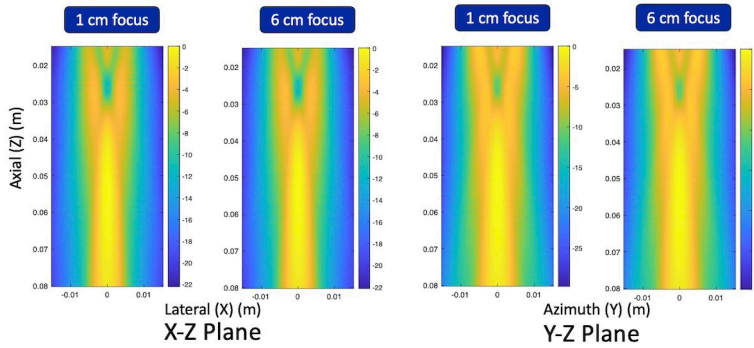

Figure 3.
X-Z and Y-Z plane simulation of beam patterns of the 6-element array at different focal depths. Color bar units are in decibels with respect to the maximum.

12-element Array: Focal Range Control for X-Z Plane and Y-Z Planes

In contrast to the 6-element array's inability to control its focal distance, the 12-element array increases the number of elements along a line through the origin to four. Due to the increase in elements in a line through the origin, a delay profile can be implemented to exhibit a concave curvature, which enhances beam focusing. In the graph, note the black dots that indicate the points of highest beam intensity. These points illustrate how the focal depth progresses as the distance increases. In **Figure 4**, when the focus is set to 1 cm, the beam is focused at 1 cm as expected. However, as the focal distance progresses beyond 35 mm, it is observed that the beam is unable to focus past this approximate far-field transition point defined by Fourier Optics (D^2/4*wavelength).

In the Y-Z Plane in **Figure 4**, the same behavior as stated for the X-Z plane is seen in the Y-Z plane. The beam's focus can be controlled to 35 mm.

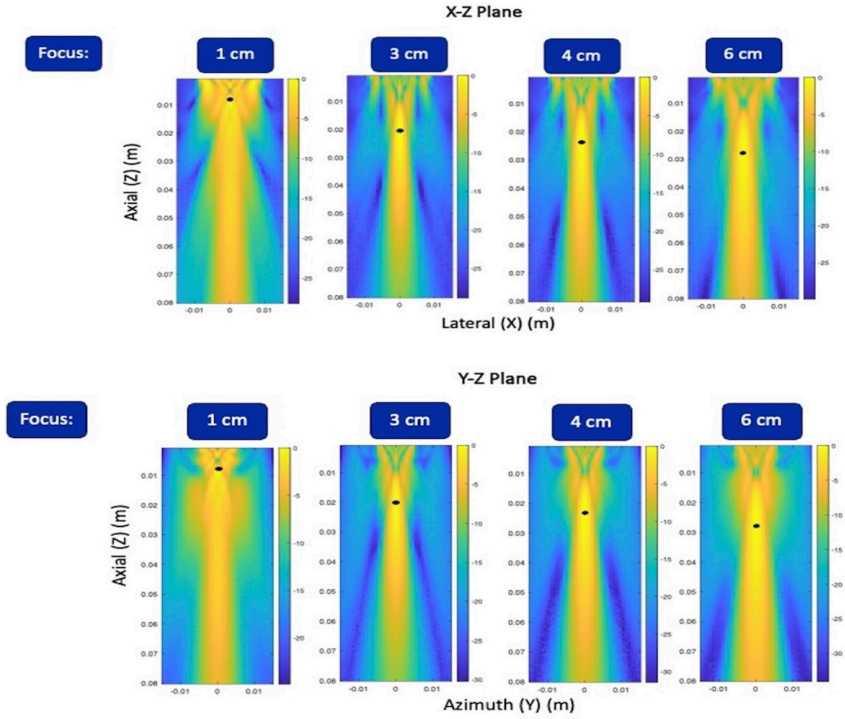

Figure 4.
X-Z Plane (top) and Y-Z Plane (bottom) simulation of beam patterns of 12 element array at varying focal depths. Color bar units are in decibels with respect to the maximum.

12-element Array: X-Y Planes at Beam Maximum

Additionally, in **Figure 5**, simulations were run to determine the maximum of the beam that could be focused. In the figures below, the X-Z plane and X-Y planes are displayed with the beam pattern perpendicularly sliced in the X-Y plane. The slices were taken in the X-Y plane at 5 mm and 35 mm.

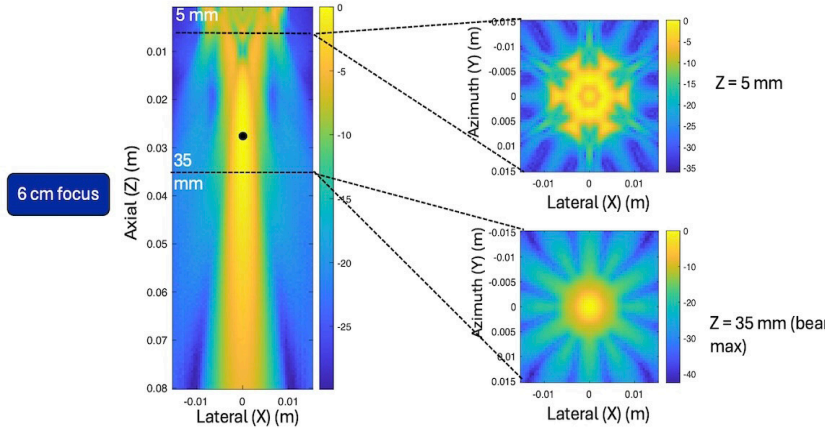

Figure 5.
The X-Z plane and X-Y planes are shown with a focus at 6 cm. Color bar units are in decibels with respect to the maximum.

12-element Array: Individual Element Response

Individual element positions were examined to understand how the beam simulates shallow focusing. From this analysis, the beam was able to deliver energy up to a depth of 1 cm, remaining reasonably laterally localized at that depth. Based on these results, it can be concluded that the array elements can effectively sample the near field. In Figure 6, the X-Z plane shows that after the simulation reaches -6-decibels at 1 cm, the 6-decibel falloff occurs beyond 1 cm. This suggests that the beam maintains a strong focus up to 1 cm, which after, the signal weakens by 6 dB. relative to the strongest intensity. A depth of 1 cm is required because the width of the acoustic window is, on average, 1 cm.

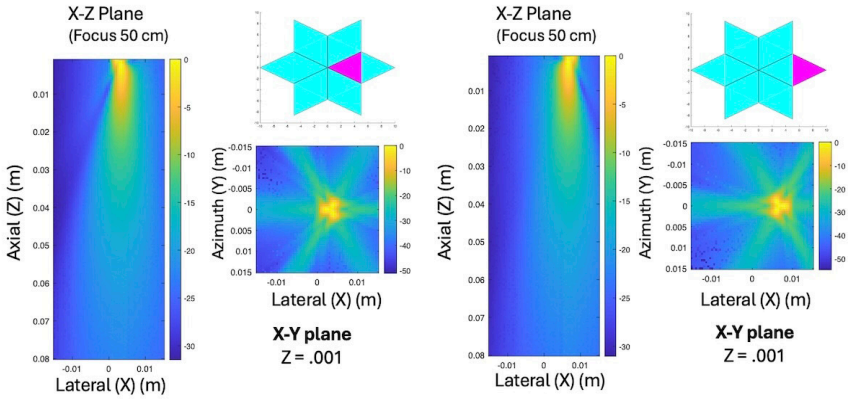

Figure 6.
Apodization of elements to characterize individual element response

12-element Array: Steering 10° Off Axis

The beam is steered 10 degrees off-axis in **Figure 7**. Grating lobes, or energy peaks off-axis to the main (steered) beam in **Figure 7**, are less than -6 decibels, indicating that the receive beam can be sufficiently steered and focused at different off-axis angles.[6] At Z=35 mm, the beam is effectively steered off axis.

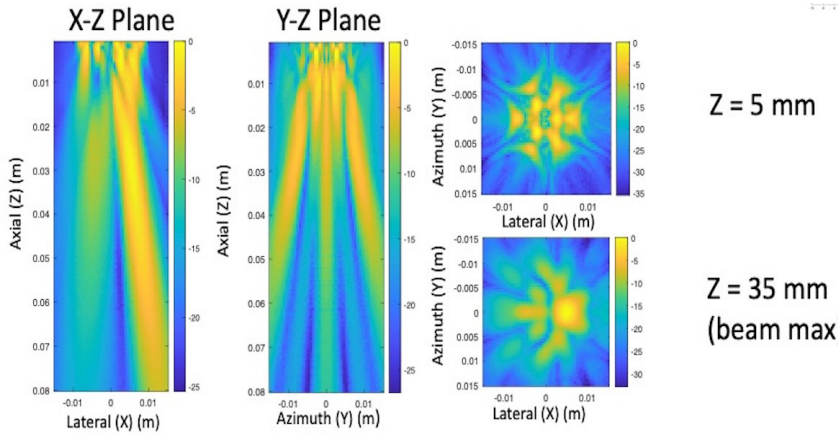

Figure 7.
X-Z, Y-Z, and X-Y plane simulations of the beam steered 10 degrees off axis. Color bar units are in decibels with respect to the maximum.

These results demonstrate the potential capabilities of a unique transducer array geometry designed for rapid stroke detection. A fundamental limitation was observed in the focal range, which is constrained to 35 mm. However, the array exhibited reasonable and useful beam shapes for the whole array whether on-axis, steered, or with individual elements. The array's basic capabilities include a focal depth of 35 mm, the ability to steer the beam off axis, and the capability to sample the near field. While the data displayed is preliminary, the final array design may require more elements to optimize its performance.

Future Work

In future work, the goal is to simulate a mock field of vessels at on-axis and off-axis locations to adjust the receive beam to detect a greater presence of flow at different angles. In this study we have only simulated the pressure fields. Vector velocity processing will also need to be conducted to improve sensitivity. An acoustic window-finding algorithm will need to be derived from experimental data. It should also be noted that the initial array geometries investigated here are not necessarily a final design; it may be necessary to increase the number of array elements to improve steering and focusing, or to more accurately measure flow density. This depends on the to-be-experimentally-derived algorithm, and how finely spaced it needs the array elements to be.

Conclusion

In summary, a simplified 2D array transducer can be constructed to provide TCD users with feedback on trends in underlying skull thickness and beam alignment with a major cerebral vessel to aid in optimal signal acquisition. This means that the 2D array can steer and focus the ultrasound beam in different directions and at varying focal depths. The Field II simulations of the 12-element triangular transducer displayed the ability to sample the near field (insonify shallow skull at different lateral locations) and control the beam focus angle (flow). However, the 6-element transducer design was less effective due to an insufficient number of elements along the axis through the origin. With the 12-element transducer design the beam could be focused and steered to different ranges ([1:1:6] mm) and angles (10°), making it a promising design that has the potential to improve LVO stroke detection at the point-of-care.

Acknowledgment

The authors sincerely thank Dr. Mark Rubin, Dr. Brent Hoffmeister, and Dr. Gianmarco Pinton for their collaboration on this project. The authors also acknowledge Kashta Dozier-Muhammad, Taylor Christian, Estefania Viloria, for their related work on this project. Thank you to Dr. Samuel Johnson, my father and primary inspiration behind my interest in medical research. The funding source for this project is the NIH/NIBIB grant R15EB034185.

References

[1] Virani, S. S., Alonso, A., Aparicio, H. J., Benjamin, E. J., Bittencourt, M. S., Callaway, C. W., Carson, A. P., Chamberlain, A. M., Cheng, S., Delling, F. N., Elkind, M. S. V., Evenson, K. R., Ferguson, J. F., Gupta, D. K., Khan, S. S., Kissela, B. M., Knutson, K. L., Lee, C. D., Lewis, T. T., Liu, J., … American Heart Association Council on Epidemiology and Prevention Statistics Committee and Stroke Statistics Subcommittee (2021). Heart disease and stroke statistics-2021 update: A report from the American heart association. *Circulation*, *143*(8), e254–e743. https://doi.org/10.1161/CIR.0000000000000950

[2] Malhotra, K., Gornbein, J., & Saver, J. L. (2017). Ischemic strokes due to large-vessel occlusions contribute disproportionately to stroke-related dependence and death: A review. *Frontiers in neurology*, *8*, 651. https://doi.org/10.3389/fneur.2017.00651

[3] Sekerdag, E., Solaroglu, I., & Gursoy-Ozdemir, Y. (2018). Cell death mechanisms in stroke and novel molecular and cellular treatment options. *Current Neuropharmacology*, *16*(9), 1396–1415.

[4] Luijten, S. P. R., Wolff, L., Duvekot, M. H. C., van Doormaal, P.-J., Moudrous, W., Kerkhoff, H., Lycklama a Nijeholt, G. J., Bokkers, R. P. H., Yo, L. S. F., Hofmeijer, J., van Zwam, W. H., van Es, A. C. G. M., Dippel, D. W. J., Roozenbeek, B., & van der Lugt, A. (2022). Diagnostic performance of an algorithm for automated large vessel occlusion detection on CT angiography. *Journal of NeuroInterventional Surgery*, *14*(8), 794–800. https://doi.org/10.1136/neurintsurg-2021-017842

[5] Purkayastha, S., & Sorond, F. (2012). Transcranial Doppler ultrasound: technique and application. *Seminars in Neurology*, *32*(4), 411–420. https://doi.org/10.1055/s-0032-1331812.

[6] Barthez, P. Y., Léveillé, R., & Scrivani, P. V. (1997). Side lobes and grating lobes artifacts in ultrasound imaging. *Veterinary Radiology & Ultrasound: The Official Journal of the American College of Veterinary Radiology and the International Veterinary Radiology Association*, *38*(5), 387–393. https://doi.org/10.1111/j.1740-8261.1997.tb02104.x